Available online at www.sciencedirect.com
SCIENCE DIRECT
Polymer 46 (2005) 11085–11092
polymer
www.elsevier.com/locate/polymer

Investigation on the early and late stage phase-separation dynamics of poly(methyl methacrylate)/poly(α-methyl styrene-*co*-acrylonitrile) blends through rheological and scattering functions

Min Zuo[a], Mao Peng[a], Qiang Zheng[a,b,*]

[a]*Department of Polymer Science and Engineering, Zhejiang University, Hangzhou 310027, People's Republic of China*
[b]*State Key Laboratories of Fluid Power Transmission and Control Institute of Mechatronic Control Engineering, Zhejiang University, Hangzhou 310027, People's Republic of China*

Received 24 April 2005; received in revised form 12 August 2005; accepted 6 September 2005
Available online 23 September 2005

Abstract

The phase-separation behavior of poly(methyl methacrylate)/poly(α-methyl styrene-*co*-acrylonitrile) (PMMA/α-MSAN) blends with two different compositions was studied by time-resolved small angle light scattering (SALS) in the spinodal decomposition (SD) regime from 160 to 210 °C. The rheological function (WLF-like equation) was introduced into the processing of light scattering data. It was found that the WLF-like equation was applicable to describe the temperature dependence of apparent diffusion coefficient D_{app} and the relaxation time τ of normalized scattering intensity $(I(t)-I(0))/(I_m-I(0))$ at the early stage of SD, as well as the relaxation time τ of maximum scattering intensity I_m and characteristic scattering vector q_m with I_m at the late stage of SD for PMMA/α-MSAN blends with two different compositions. This is in consistence with the phase-separation behavior of PMMA/SAN reported in our previous paper.

Keywords: PMMA/α-MSAN blends; Spinodal decomposition; WLF-like function

1. Introduction

It is well-known that the properties of multi-component/multi-phase polymer mixtures depend mainly on their phase structure/morphology. In the last several decades, phase separation behaviors of polymer mixtures having the low critical solution temperature (LCST) or upper critical solution temperature (UCST) have attracted a great many researchers' attention [1–3]. Investigations on the mechanism and kinetics of nucleation and growth (NG) and spinodal decomposition (SD) phase-separation by experiments [4–10], theoretical analysis [11–14] and computer simulations [15–17] have been carried out extensively. The sufficient understanding to the phase-separation behavior of multi-component/multi-phase polymer mixtures helps us optimize the phase structure, domain size, and then the mechanical properties.

The phase morphologies of polymer blends can be characterized by using many different methods such as optical microscopy, atomic force microscopy (AFM) [18,19], X-ray photoelectron spectroscopy (XPS) [19,20], magnetic resonance imaging (MRI) [21] and small angle light scattering (SALS) [4–6,22], etc. For its ability to determine the weak concentration fluctuation and fine domain size at the early stage of phase separation, SALS is a powerful and conventional method in the study of phase-separation mechanism and kinetics, provided the polymer pair differ enough in refractive index. Cahn [23] predicted the exponential growth of a scattering intensity during SD, which has been confirmed to be true in some metal alloys, glasses, liquids and also in many polymer blends [24–27]. The results by Langer et al. [28] and Binder et al. [29] evidenced that at the late stage the time-dependent scattering significantly deviates from exponential growth but follows a power-law scheme.

In studying the SD behavior of polymer mixtures, we are especially interested in the measurement of equilibrium SD temperature (T_{SD}). According to Hashimoto [4], the apparent diffusion coefficient $D_{app}(T)$ exhibits linear dependence to temperature when approaching the equilibrium T_{SD}, and T_{SD} can be determined to be the temperature at which $D_{app}(T)$ can

* Corresponding author. Address: Department of Polymer Science and Engineering, Zhejiang University, Hangzhou 310027, People's Republic of China. Tel.: +86 571 87952522; fax: +86 571 87952522.
E-mail address: zhengqiang@zju.edu.cn (Q. Zheng).

0032-3861/$ - see front matter © 2005 Elsevier Ltd. All rights reserved.
doi:10.1016/j.polymer.2005.09.017

be linearly extrapolated to zero. This was found to be valid for some systems [5,6]. However, for some other polymer pairs which T_{SD} were close to their glass transition temperatures (T_g), the linear region was difficult to be identified [4,8] and the temperature dependence of $D_{app}(T)$ over a wide temperature range has not been paid enough attention. In our previous works [22,30], we investigated the SD behavior of the poly(methyl methacrylate)/poly(styrene-*co*-acrylonitrile) (PMMA/SAN) mixtures over a relatively wide temperature range. It was found that $D_{app}(T)$ exponentially depends on temperature, and can be well described by using the time-temperature superposition (TTS) principle and Williams-Landel-Ferry (WLF) function. More recently, Li et al. [31,32] found that the TTS principle is also applicable to reaction induced phase-separation kinetics of thermosetting/thermoplastic mixtures.

As is well known, the TTS principle and WLF function are used to describe the temperature dependence of viscoelastic responses, mechanical and electrical relaxations of unitary systems, such as amorphous polymers, polymer solutions, organic glass-forming liquids and inorganic glasses. This arises from the fact that the rates of all such processes depend on temperature primarily in terms of their dependence on free volume [33]. As to the multi-component systems, their dependence of free volume on temperature should be more complicated, and presently, TTS principle and WLF function are seldom used by researchers to describe the phase-separation behavior of binary polymer blends. Hence, there should be more experiment evidence to confirm the applicability of the WLF function in multi-component/multi-phase polymer systems.

It has been reported that the relaxation time of amorphous polymers controlled by diffusion of segments and the temperature dependence of segment diffusion follow the TTS principle in the glass transition region [34,35]. Hence, we believe that the viscous diffusion of macromolecules chains during phase-separation plays an important role in the phase separation kinetics.

In this article, we selected another binary mixture composed of poly(methyl methacrylate) (PMMA) and poly(α-methyl styrene-*co*-acrylonitrile) (α-MSAN) as a model system, a similar system to that in our previous works, and explored their phase-separation behavior through examining the time evolution of scattering intensity at various stages of SD and the temperature dependence of $D_{app}(T)$ during isothermal annealing. The aim is to explore the applicability of TTS principle and a WLF-like equation to describe the temperature dependence of $D_{app}(T)$ and the relaxation time τ of scattering intensity I at the early or late stage of SD for PMMA/α-MSAN blends, and to understand whether the phase-separation behavior of this system also follows the TTS principle; in other words, whether the TTS principle could be applied to other polymer blends or not. We believe this study, together with our previously reported results will help us better understand the importance of TTS principle and WLF function to the phase separation behavior of binary polymer mixtures. Furthermore, the investigated temperatures range from 160 to 210 °C, because the samples are stable and their phase separation rate is appropriate for observation within this range. Applicability of TTS principle and WLF function to the phase separation behavior of binary polymer mixtures is potentially helpful for us to control the processing temperature and optimize the phase structure, domain size, and then the mechanical properties.

2. Experimental

2.1. Materials and sample preparation

Poly(methyl methacrylate) (PMMA) (IF850, $M_w = 8.0 \times 10^4$, $M_w/M_n = 2.1$, LG Co. Ltd, South Korea) and poly(α-methyl styrene-*co*-acrylonitrile) (α-MSAN) (Luran KR 2556, $M_w = 9.5 \times 10^4$, $M_w/M_n = 2.2$, BASF Co. Ltd, Germany) with AN content of 32 wt% were both commercial products and used as received. PMMA and α-MSAN at two weight ratios of 60/40 and 40/60 were dissolved in methyl ethyl ketone (MEK) (C_4H_8O) at 5% by weight to form a clear and uniform solution. The solution was then cast on the surface of cover glasses of 25 °C. After the solvent evaporated at an ambient environment, the samples were further dried at 90, 110, 130 °C, respectively, in a vacuum oven for at least 72 h to remove residual solvent. The thickness of the sample film was measured to be about 20–25 μm with uniform and transparent appearance, characteristic of single-phase structure.

2.2. Glass transition temperature measurement

The glass transition temperature (T_g) of PMMA/α-MSAN blends was measured by using advanced rheometric extension system (ARES). The rectangular samples have the length, width, and thickness of 30.0, 12.0 and 1.5 mm, respectively. The heating rate and the frequency in dynamic rheological measurements were 2 °C min^{-1} and 10 rad s^{-1}, respectively.

2.3. Time-resolved small-angle light scattering (SALS)

The time-resolved small-angle light scattering apparatus was the same as that used in our previous paper [22,30]. The principle and details of the SALS system were available in the literature [4,36,37]. Three milliwatt He–Ne laser generator was used as the incident beam with the wavelength of 632.8 nm. The hot stage controlled by an intelligent controller (AI-708, YUGUANG, Xiamen) has a temperature accuracy of about ± 0.1 °C. The scattering pattern was detected by a CCD digital camera (MTV-12V1C, MINTRON, Taiwan, ROC) and imported into the computer memory in real time through a video capturing board (VIDEO VESA CG-400, Daheng, Beijing). Online circular averaging of each scattering pattern was performed to obtain the relationship between intensity and scattering angle. The intensity at the beginning of examination was subtracted from the intensity measured at later time as background to avoid the negative effects of parasitic light, thermal fluctuation and the dark current of CCD camera.

3. Theoretical background

Cahn and Hilliard [38] described the free energy F of a heterogeneous binary mixture composed of small molecules in the incompressible limit as

$$F = \int \mathrm{d}v[f(\phi) + k(\nabla\phi)^2 + L] \tag{1}$$

where $f(\phi)$ is free energy density of the system having composition ϕ of one component which is uniform everywhere in space and the second item is the excess free energy arising from a concentration gradient. The quantity ϕ refers to volume fraction of one of the components. k is the energy gradient coefficient arising from contributions of composition gradient to the energy. At the early stage of decomposition, the diffusion function is as follows:

$$\frac{\partial\phi}{\partial t} = M\left[\left(\frac{\partial^2 f}{\partial\phi^2}\right)\nabla^2\phi - 2k\nabla^4\phi + L\right] \tag{2}$$

where M is the mobility coefficient of molecules.

The solution of Eq. (2) is obtained by

$$\phi(\vec{r}) - \phi_0 = \sum_q \exp[R(q)t]\{A(q)\cos(q\cdot\vec{r}) + B(q)\sin(q\cdot\vec{r})\} \tag{3}$$

The relaxation rate or amplification factor $R(q)$ is further related by

$$R(q) = -Mq^2\left(\frac{\partial^2 f_\mathrm{m}}{\partial\phi^2} + 2kq^2\right) \tag{4}$$

where f_m is the mean field free energy of mixing, $q = 4\pi/\lambda\sin(\theta/2)$ is the wavenumber of the spatial composition fluctuation, λ is the corresponding wavelength and θ is the scattering angle. From the above equation, the intensity evolution at the initial stage of phase separation can be calculated, that is the Cahn–Hilliard function [23]. Considering the thermal fluctuation of stable binary polymer blends, Cook [24] modified the Cahn-Hilliard function into

$$I(q,t) = I_\mathrm{s}(q,0) + [I(q,0) - I_\mathrm{s}(q,0)]\exp[2R(q)t] \tag{5}$$

in which $I_\mathrm{s}(q,0)$ is the scattering intensity of the stable system.

Eq. (4) includes the apparent diffusion coefficient D_app, which describes the uphill diffusion during spinodal decomposition.

$$D_\mathrm{app} = -M\frac{\partial^2 f_\mathrm{m}}{\partial\phi^2} \tag{6}$$

From Eq. (5), it is obvious that plots of $\ln[(I(q,t) - I_\mathrm{s}(q,0))/(I_\mathrm{m}(q,t_\mathrm{m}) - I_\mathrm{s}(q,0))]$ vs. t yields $R(q)$ and then from Eqs. (4) and (6), the D_app and $2Mk$ values can be obtained from the intercept and slope of the plot of $R(q)/q^2$ vs. q^2.

Differentiation of Eq. (6) with respect of q yields the characteristic scattering vector q_m with I_m at the early stage of phase separation, the scattering vector corresponding to the correlation length of maximal growth $\Lambda = 1/q_\mathrm{m}$, which is no function of time as related by:

$$q_\mathrm{m}(t=0) = \sqrt{\frac{D_\mathrm{app}}{4Mk}} \tag{7}$$

In the late stage of SD, the prevalent mechanism is the nonlinear phase growth that causes the scattering halo to shrink to a smaller diameter, which is the coarsening process of the phase domains. This process follows the power laws, in which the time evolution of q_m and $I(q_\mathrm{m})$ in the late stage is described as [27,29]

$$I(q_\mathrm{m}(t)) \propto t^{\beta} \tag{8}$$

$$q_\mathrm{m}(t) \propto t^{-\alpha} \tag{9}$$

4. Results and discussion

4.1. Glass transition temperature (T_g)

The temperature dependence curves of loss tangent (tan δ) for PMMA, α-MSAN, PMMA/α-MSAN (60/40) blend and PMMA/α-MSAN (40/60) blend are presented in Fig. 1. The glass transition temperature of PMMA, α-MSAN PMMA/α-MSAN (60/40) blend and PMMA/α-MSAN (40/60) blend are 109, 130.9, 119.7 and 123.6 °C, respectively. Only a single T_g for both PMMA/α-MSAN (60/40) blend and PMMA/α-MSAN (40/60) blend can be observed, indicating the existence of the single phase in the mixtures prepared by solvent casting; otherwise, two independent tan δ peak should be observed.

4.2. Time evolution of scattering intensity during isothermal annealing

Light-scattering results are presented only for two compositions of 60/40 and 40/60 because their scattering light is strong enough and phase separation temperature range is appropriate for detection. The scattering intensity $I(t)$ at given scattering vector $q(t)$, is normalized as $(I(t) - I(0))/(I_\mathrm{m} - I(0))$, in which $I(0)$ is the intensity at the start of experiment and I_m is

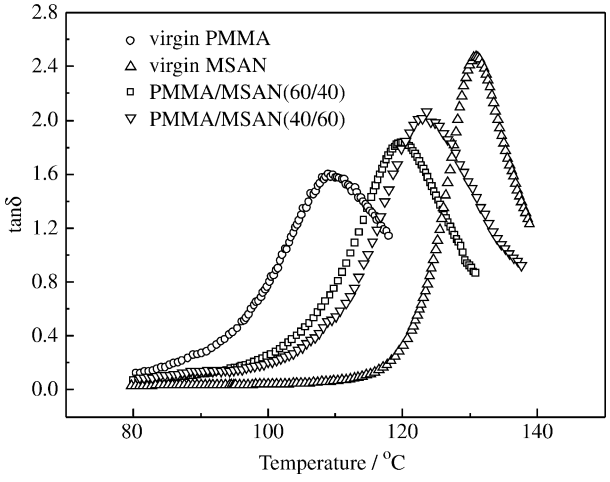

Fig. 1. Temperature dependence of loss tangent (tan δ) for virgin PMMA, α-MSAN, PMMA/α-MSAN (60/40) blend and PMMA/α-MSAN (40/60) blend.

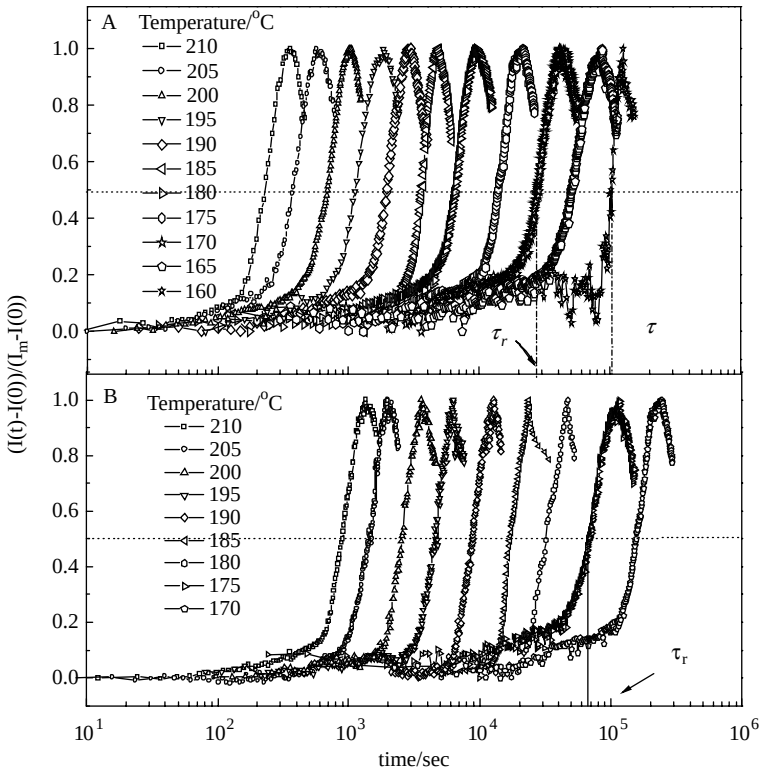

Fig. 2. Time evolution of normalized scattering intensity of PMMA/α -MSAN blends: (A) 60/40 blends and (B) 40/60 blends at $q=6.6\ \mu m^{-1}$ under different annealing temperatures.

the maximum value of $I(t)$ during thermal annealing process, in order to make a reliable comparison of the time evolution of scattering light for various temperatures and avoid the negative effect of the sample diversity resulted from the concentration inhomogeneity and thickness difference for various samples.

Fig. 2 shows the semilogarithmic plots of normalized scattering light intensity versus time at $q=6.6\ \mu m^{-1}$, during isothermal annealing process under various temperatures. It is interesting to note that for both compositions, all curves at different temperatures are nearly similar and parallel to each other, implying that they can superpose with each other and then form a master curve by horizontal shifting. This suggests that the TTS principle is applicable to this system as same as PMMA/SAN which was reported previously by us [30].

For the PMMA/α-MSAN (60/40) blends, taking 170 °C as the reference temperature T_r, being 50 °C higher than their glass transition temperature T_g, shifting factor $a_T=\tau/\tau_r$, can be obtained from Fig. 2(A), in which τ is the relaxation time at which the normalized scattering intensity for different annealing temperatures increases by the same degree, for instance 50%, as is shown in Fig. 2(A), τ_r is the relaxation time at the reference temperature 170 °C. The temperature dependence of a_T is presented in Fig. 3. It can be founded that a_T decreases exponentially with the increase of temperature and the plots of $(T-T_r)/\log \alpha_T$ against $(T-T_r)$ at temperatures higher than 170 °C nearly exhibit a linear relationship. Hence, the temperature dependence of a_T can be described as the WLF function:

$$\log a_T = \log \frac{\tau}{\tau_r} = \frac{-C_1(T-T_r)}{C_2+T-T_r} \tag{10}$$

in which the constants C_1 and C_2 are 8.30 and 121.5 °C, respectively. It is found that the values of C_1 and C_2 are very close to the empirical constants, 8.86 and 101.6 °C of the universal WLF function for polymer melt viscosity, respectively, at the reference temperature of 50 K higher than T_g. For

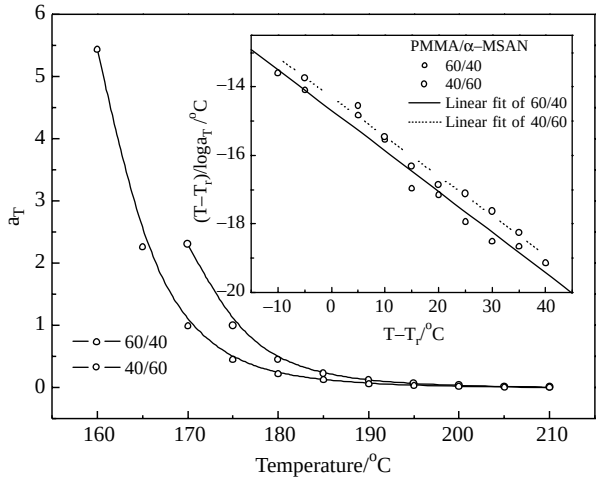

Fig. 3. Relationship between shifting factor a_T and temperature for PMMA/α-MSAN blends: 60/40 blends (△), 40/60 blends (□). The inlay presents the $(T-T_r)/\log a_T$ relationship, respectively, at the corresponding reference temperatures.

the PMMA/α-MSAN (40/60) blends, taking 175 °C as the reference temperature T_r, the relaxation time τ of I_m was obtained in the temperature range from 170 to 210 °C. It is found that a very similar result can be obtained with the constants C_1 and C_2 values being 8.66 and 123.8 °C, respectively, as shown in Fig. 2(B) and Fig. 3. These results are very close to those for the PMMA/α-MSAN (60/40) blends. The results for the two kinds of blends with different compositions indicate that the phase-separation behaviors of PMMA/α-MSAN system follow the TTS principle. The time evolution of scattering intensity at several other vectors within the region of from 1.5 to 8.0 μm^{-1} also keeps to the principle. Therefore, it can be concluded that for all scattering vectors in the observation the TTS principle can be applied to this polymer blend.

4.3. Time evolution of scattering profiles during the early stage of SD

Fig. 4 shows change of the scattering intensity with time at various q for PMMA/α-MSAN (60/40) blends at 185 °C. The scattering vector q_m with the maximum scattering intensity, does not vary with time at the early stage of phase separation and then decreases with time, whereas the scattering intensity increases within the whole process, which indicates that the phase-separation behavior of PMMA/α-MSAN (60/40) blends follows the characteristic of spinodal decomposition (SD).

Fig. 5 presents that the semilogarithmic plots of the normalized scattering intensity vs. time for different scattering vectors from 5.6 to 7.9 μm^{-1} at 175 °C show satisfactory linearity at the early stage of SD. According to the Eq. (5), the relaxation rate $R(q)$, as a function of the scattering vector q of the spatial fluctuations, can be calculated from the initial slope

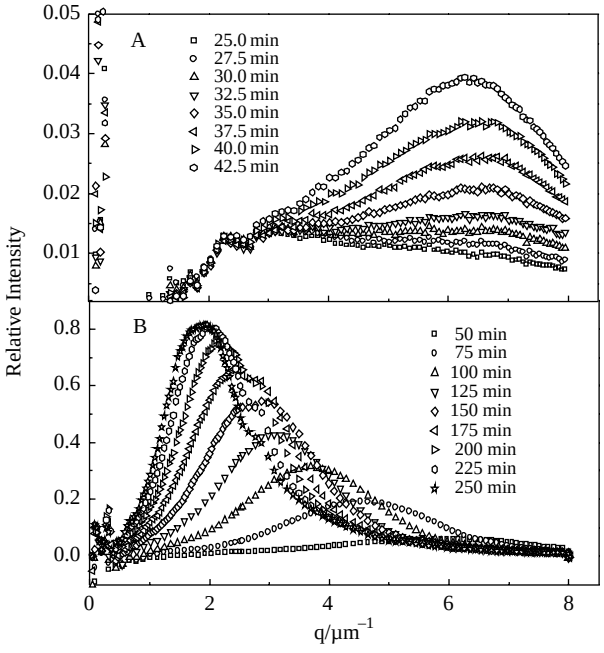

Fig. 4. The evolution of the relative intensity versus q for PMMA/α-MSAN (60/40) blend at 185 °C during the early (A) and late (B) stages.

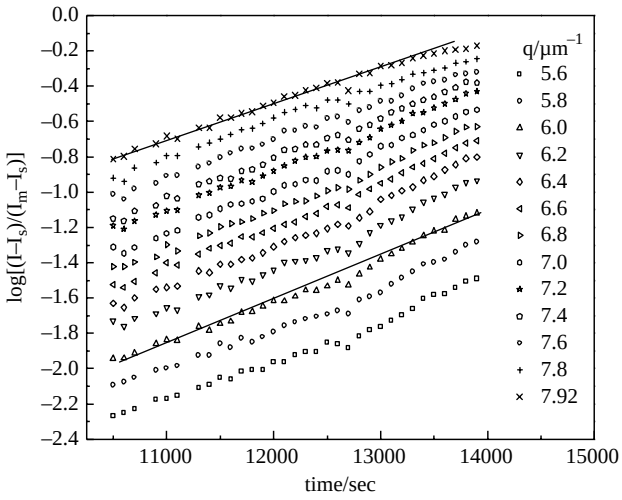

Fig. 5. Time evolution of $\log[(I-I_s)/(I_m-I_s)]$ for PMMA/α-MSAN (60/40) blends at various scattering vectors (5.6–7.9 μm^{-1}) under 175 °C during the early stage of phase separation.

of $\ln[(I(t)-I(0))/(I_m-I(0))]$ vs. t. Then in correspondence with Eq. (4), $R(q)/q^2$ were plotted against q^2 in Fig. 6(A) and (B), and D_{app} and $2Mk$ can be obtained from the intercepts and slopes of those plots. In the observation temperature region, the plots of $R(q)/q^2$ vs. q^2 follow linear relationship well at large q values, close to the q_m, which indicates that this stage of spinodal decomposition can be well described by the linearized Cahn–Hilliard theory. At small q values, the plots deviate from the linear function, hence only the plots at large q values are shown in Fig. 6. It is obvious that the relaxation rate $R(q)$

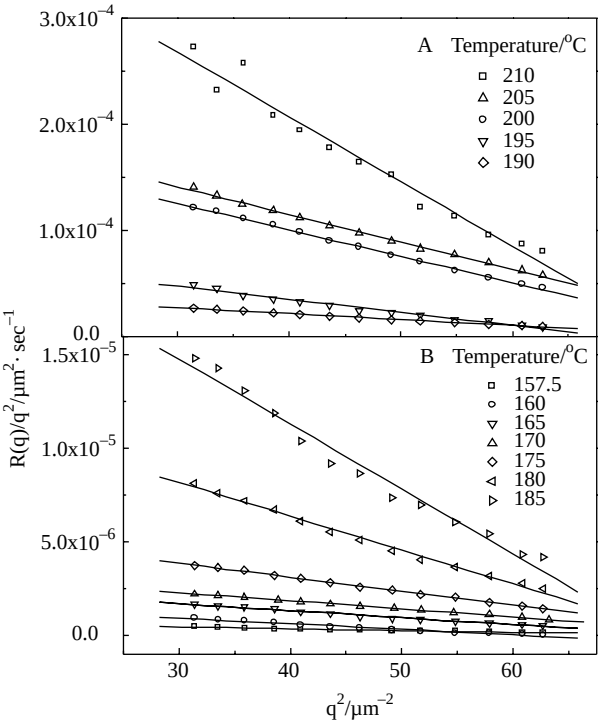

Fig. 6. Relationships between $R(q)/q^2$ and q^2 for PMMA/α-MSAN (60/40) blends (A) at high annealing temperatures and (B) at low annealing temperatures.

increases with the increase of temperature. The relationship between $R(q)/q^2$ and q^2 of the PMMA/α-MSAN (40/60) blends are similar to those of PMMA/α-MSAN (60/40) blends. According to the Eq. (7), the above-obtained D_{app} and $2Mk$ can be used for a consistency check of the scattering data, because it should be similar to the experimental q_m value. Fig. 7 gives a comparison between the temperature dependence of experimental q_m and the theoretical values calculated by using Eq. (7). It is found that the theoretical values satisfactorily agree with the experimental data (with error smaller than 5%), which indicates that the D_{app} and $2Mk$ values obtained from light scattering experiment are reliable. It is interesting that q_m is almost independent of temperatures investigated, similar to the results of other systems reported by Edel previously [5].

Figs. 8(A) and (B) demonstrate that the plots of D_{app} and $2Mk$ for PMMA/α-MSAN (60/40) blends and PMMA/α-MSAN (40/60) blends as a function of temperature show nearly exponential behavior in the given temperature range, the inlays in which show the linear functions for $(T-T_r)/\log(D_{app}(T_r)/D_{app}(T)) \sim (T-T_r)$ and $(T-T_r)/\log(2Mk(T_r)/2Mk(T)) \sim (T-T_r)$, where the reference temperatures are the same as those mentioned in Section 4.2. It can be seen that the WLF-like function is also applicable to describe the temperature dependence of $D_{app}(T)$ and $2Mk(T)$ for two systems, just like a_T of relaxation time. The constants of PMMA/α-MSAN (60/40) blends in the WLF-like function of $D_{app}(T)$ and $2Mk(T)$ calculated from the interceptions and slopes of the above two linear plots are $C_1=8.85$, $C_2=124.5$ °C and $C_1=8.02$, $C_2=112.7$ °C, respectively. Furthermore, those of PMMA/α-MSAN (40/60) blends are $C_1=8.55$, $C_2=97.5$ °C and $C_1=9.0$, $C_2=106.2$ °C, we obtain the WLF-like function of $D_{app}(T)$ and $2Mk(T)$ as follows:

$$\log\frac{D_{app}(T_r)}{D_{app}(T)} = -\frac{C_1(T-T_r)}{C_2+T-T_r} \tag{11}$$

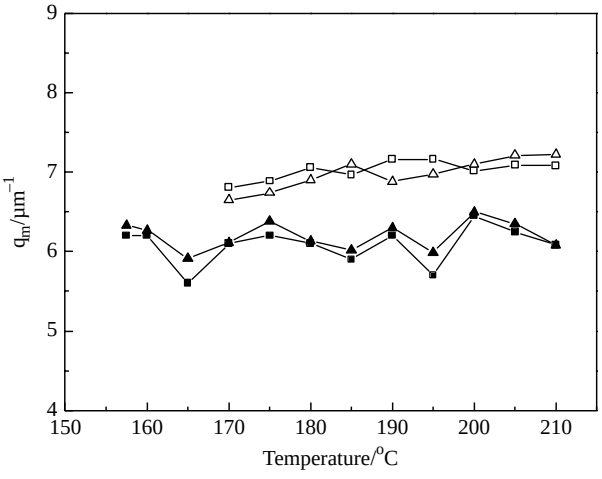

Fig. 7. Temperature dependence of scattering vector with maximum intensity q_m for PMMA/α-MSAN blends: 60/40 blends (solid symbols) and 40/60 blends (open symbols); experimental values (□) and theoretical values (△) calculated by using Eq. (7).

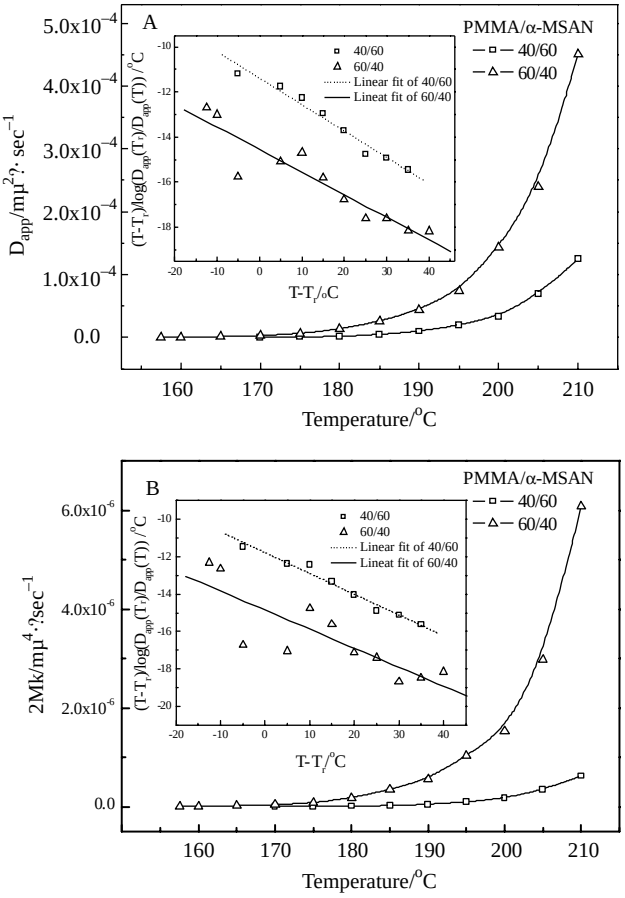

Fig. 8. Temperature dependence of (A) $D_{app}(T)$ and (B) $2Mk(T)$ for PMMA/α-MSAN blends: 60/40 blends (△), 40/60 blends (□). The inlays present the $(T-T_r)/\log(D_{app}(T_r)/D_{app}(T)) \sim (T-T_r)$ and $(T-T_r)/\log(2Mk(T_r)/2Mk(T)) \sim (T-T_r)$ relationship, respectively, at the corresponding reference temperatures.

$$\log\frac{2Mk(T_r)}{2Mk(T)} = -\frac{C_1(T-T_r)}{C_2+T-T_r} \tag{12}$$

4.4. Time evolution of scattering profiles during the late stage of SD

In order to obtain the comprehensive parameters characterizing the kinetics of SD over a wide time scale, including both the early and late stage, the maximum scattering intensity I_m and the characteristic scattering vector q_m with I_m for PMMA/α-MSAN (60/40) blends and PMMA/α-MSAN (40/60) blends are plotted as a function of time in Fig. 9(A) and (B). In the late stage of SD, q_m starts to decrease with time. Namely, the characteristic wavelength of the spatial composition fluctuations increase with time and I_m starts to deviate from the exponential increase with time in such a way that the rate of the intensity increase intends to slow down, when the kinetics starts to deviate from the linear Cahn–Hilliard theory and be affected by the coarsening effect. It is found that for these two systems, both q_m and I_m follow the power law; moreover, the relationships between exponents α and β follow

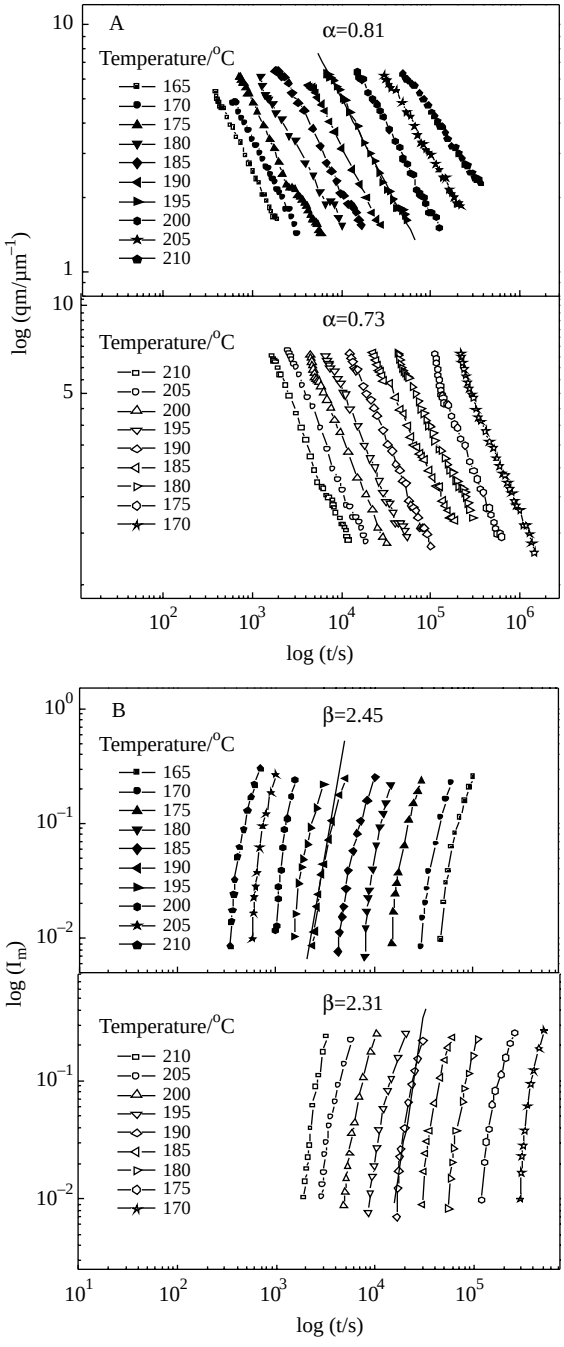

Fig. 9. Time evolution of (A) q_m and (B) I_m for PMMA/α-MSAN blends: 60/40 blends (solid symbols) and 40/60 blends (open symbols) at the late stage of SD under various temperatures.

$\beta = 3\alpha$ at all the temperatures investigated, which accords with Siggia's theory for most binary polymer blends [26].

Similar to the above-mentioned plot of $(I(t)-I(0))/(I_m-I(0)) \sim t$ at various temperatures, $\log I_m \sim \log t$ and $\log q_m \sim \log t$ plots at different temperatures are parallel with each other and may be reduced to a master curve by horizontal shifting, suggesting that the TTS principle is also applicable. According to the arithmetic mentioned in the Section 4.2, the shifting factors $a_T(q_m)$ and $a_T(I_m)$ for q_m and I_m can be obtained from the Fig. 9(A) and (B), setting 170 °C as the reference temperature. The plots of $(T-T_r)/\log a_T(q_m) \sim (T-T_r)$ and $(T-T_r)/\log a_T(I_m) \sim (T-T_r)$ for PMMA/α-MSAN (60/40) blends at the late stage of SD are shown in Fig. 10(A) and (B). The linear results indicate that the WLF-like function can also be applied to these relationships satisfactorily, where the constants of WLF-like function are $C_1 = 8.51$, $C_2 = 116.3$ for $(T-T_r)/\log a_T(q_m) \sim (T-T_r)$ and $C_1 = 8.45$, $C_2 = 111.3$ for $(T-T_r)/\log a_T(I_m) \sim (T-T_r)$, respectively. In the same way, the constants of WLF-like function for PMMA/α-MSAN (40/60) blends can be obtained with $C_1 = 8.43$, $C_2 = 132.6$ for $(T-T_r)/\log a_T(q_m) \sim (T-T_r)$ and $C_1 = 8.79$, $C_2 = 135.4$ for $(T-T_r)/\log a_T(I_m) \sim (T-T_r)$, respectively.

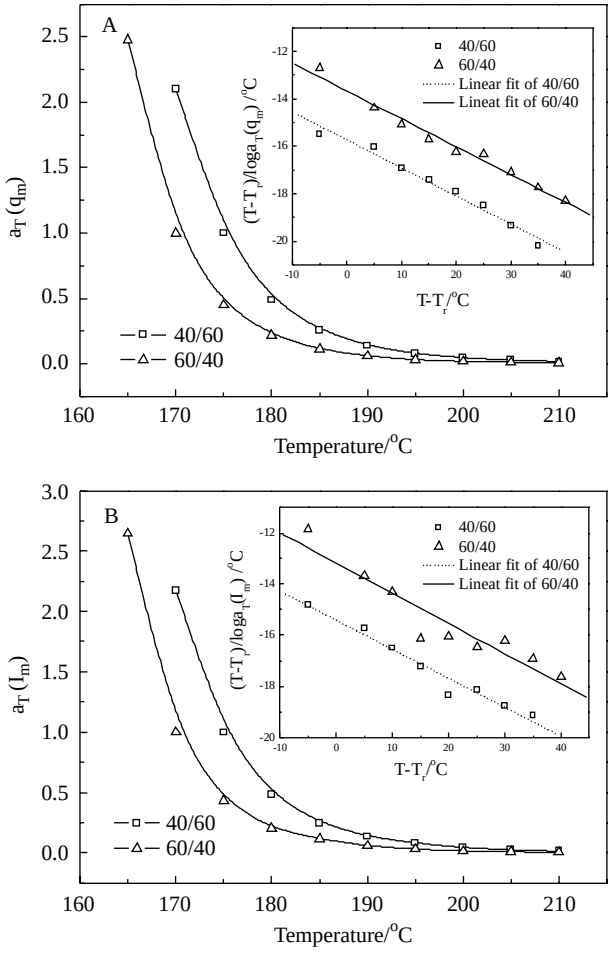

Fig. 10. The plots of (A) $(T-T_r)/\log a_T(q_m) \sim (T-T_r)$ and (B) $(T-T_r)/\log a_T(I_m) \sim (T-T_r)$ for PMMA/α-MSAN blends: 60/40 blends (△), 40/60 blends (□) at the late stage of SD.

5. Summary and remarks

We have investigated the early and later stage of phase separation behavior of PMMA/α-MSAN mixtures by using SALS apparatus in details. Similar to the PMMA/SAN mixtures as was investigated in our previous works [22,30], the temperature dependences of phase-separation kinetics for different compositions at either the early or late stage of SD both follow the TTS principle within the temperature region investigated. The Williams–Landel–Ferry (WLF) function is applicable to describe the temperature dependence of apparent

diffusion coefficient $D_{app}(T)$ and relaxation time τ of normalized scattering intensity $(I(t)-I(0))/(I_m-I(0))$ at the early stage of SD, as well as the phase behavior at the late stage of SD. This presents another powerful evidence for the applicability of the TTS principle and WLF-like function for describing the phase-separation behavior of binary polymer mixtures over a relatively large temperature range.

Acknowledgements

This work was mainly supported by the National Nature Science Funds for Distinguished Young Scholars (Grant 50125312) and National Nature Science Foundation of China (Grant 50373037).

References

[1] Paul DR, Newman S, editors. Polymer blends, vols. 1 and 2. New York: Academic Press; 1978.
[2] Olabisi O, Shaw LM, Shaw MT. Polymer–polymer miscibility. New York: Academic Press; 1979.
[3] Gunton JD, San Miguel M, Sahni PS. In: Domb C, Lebowitz J, editors. Phase transitions and critical phenomenon, vol. 8. New York: Academic Press; 1983.
[4] Hashimoto T, Kumaki J, Kawai H. Macromolecules 1983;16:641.
[5] Edel V. Macromolecules 1995;28:6219.
[6] Kyu T, Saldanha JM. Macromolecules 1988;21:1021.
[7] Bruder F, Brenn R. Phys Rev Lett 1992;69:624.
[8] Snyder HL, Meakin P. Macromolecules 1983;16:757.
[9] Lim D, Kyu T. J Chem Phys 1990;92:3944.
[10] Roe RJ, Kuo CM. Macromolecules 1990;23:4635.
[11] Binder K. J Chem Phys 1983;79:6387.
[12] de Gennes PG. J Chem Phys 1980;72:4756.
[13] Furukawa H. Adv Phys 1985;34:703.
[14] Furukawa H. Prog Theor Phys Suppl 1989;99:358.
[15] Ball RC, Essery RLH. J Phys: Condens Matter 1990;2:10303.
[16] Chakrabarti A. Phys Rev Lett 1992;69:1548.
[17] Puri S, Binder K. Phys Rev A 1992;46:R4487.
[18] Magonov SN, Elings V, Papkov VS. Polymer 1997;38:297.
[19] Wen GY, Li X, Liao YG, An LJ. Polymer 2003;44:4035.
[20] Goh SH, Lee SY, Dai J, Tan KL. Polymer 1996;37:5305.
[21] Laity PR, Glover PM, Hay JN. Polymer 2002;43:5827.
[22] Peng M, Zheng Q. Chinese J Polym Sci 2000;18:565.
[23] Cahn JW. J Chem Phys 1965;42:93.
[24] Cook HE. Acta Metall 1970;18:297.
[25] Snyder HL, Meakin P. J Chem Phys 1983;79:5588.
[26] Siggia ED. Phys Rev A 1979;20:595.
[27] Langer JS. Acta Metall 1973;21:1649.
[28] Langer JS, Baron M, Miller HS. Phys Rev A 1975;11:1417.
[29] Binder K, Stauffer D. Phys Rev Lett 1973;33:1006.
[30] Zheng Q, Peng M, Song YH, Zhao TJ. Macromolecules 2001;34:8483.
[31] Gan WJ, Yu YF, Wang MH, Tao QS, Li SJ. Macromolecules 2003;36:7746.
[32] Yu YF, Wang MH, Gan WJ, Tao QS, Li SJ. J Phys Chem B 2004;108:6208.
[33] Williams ML, Landel RF, Ferry JD. J Am Chem Soc 1955;77:3701.
[34] Wisanrakkit G, Gillham JK. J Appl Polym Sci 1990;41:2885.
[35] Christopher WW, Cook WD, Goodwin AA. Polymer 1997;38:3251.
[36] Nishimoto M, Keskkula H, Paul DR. Polymer 1989;30:1279.
[37] Parizel N, Kempkes F, Cirman C, Picot C, Weill G. Polymer 1998;39:2.
[38] Cahn JW, Hilliard JE. J Chem Phys 1958;29:258.